Picosecond 554 nm yellow-green fiber laser source with average power over 1 W

M. J. Petrasiunas,[1]* M. I. Hussain,[1] J. Canning,[2] M. Stevenson,[2] and D. Kielpinski[1]

[1]*Centre for Quantum Dynamics, Griffith University, Nathan, Queensland 4111, Australia*
[2]*Interdisciplinary Photonics Laboratories (iPL), School of Chemistry, Madsen Building F09, University of Sydney, Sydney, NSW, 2006, Australia*

*m.petrasiunas@griffith.edu.au

Abstract: We demonstrate a source of 554 nm pulses with 2.7 ps pulse duration and 1.41 W average power, at a repetition rate of 300 MHz. The yellow-green pulse train is generated from the second harmonic of a 1.11 μm fiber laser source in periodically-poled stoichiometric $LiTaO_3$. A total fundamental power of 2.52 W was used, giving a conversion efficiency of 56%.

OCIS codes: (140.3515) Lasers, frequency doubled; (060.2320) Fiber optics amplifiers and oscillators; (190.7110) Ultrafast nonlinear optics.

References and links

1. M. F. Garcia-Parajo, M. Koopman, E. M. van Dijk, V. Subramaniam, and N. F. van Hulst, "The nature of fluorescence emission in the red fluorescent protein DsRed, revealed by single-molecule detection," Proc. Natl. Acad. Sci. U.S.A. **98**, 14392–14397 (2001).
2. G. R. Castro, B. K. Larson, B. Panilaitis, and D. L. Kaplan, "Emulsan quantitation by Nile red quenching fluorescence assay," Appl. Microbiol. Biot. **67**, 767–770 (2005).
3. P. G. Pappas, M. M. Burns, D. D. Hinshelwood, M. S. Feld, and D. E. Murnick, "Saturation spectroscopy with laser optical pumping in atomic barium," Phys. Rev. A **21**, 1955–1968 (1980).
4. T. Kuwamoto, K. Honda, Y. Takahashi, and T. Yabuzaki, "Magneto-optical trapping of Yb atoms using an intercombination transition," Phys. Rev. A **60**, R745–R748 (1999).
5. H. Yu, K. Wu, H. Zhang, Z. Wang, J. Wang, and M. Jiang, "Nd:YGG crystal laser at 1110 nm: a potential source for detecting carbon monoxide poisoning," Opt. Lett. **36**, 1281–1283 (2011).
6. W. Denk, J. H. Strickler, and W. W. Webb, "Two-photon laser scanning fluorescence microscopy," Science **248**, 73–76 (1990).
7. Z. Wang, Q. Peng, Y. Bo, J. Xu, S. Xie, C. Li, Y. Xu, F. Yang, Y. Wang, D. Cui, and Z. Xu, "Yellow-green 52.3W laser at 556nm based on frequency doubling of a diode side-pumped Q-switched Nd:YAG laser," Appl. Opt. **49**, 3465–3469 (2010).
8. S. V. Kurbasov and L. L. Losev, "Raman compression of picosecond microjoule laser pulses in $KGd(WO_4)_2$ crystal," Opt. Commun. **168**, 227–232 (1999).
9. E. Granados, H. M. Pask, and D. J. Spence, "Synchronously pumped continuous-wave mode-locked yellow Raman laser at 559 nm," Opt. Express **17**, 569–574 (2009).
10. E. Granados, H. M. Pask, E. Esposito, G. McConnell, and D. J. Spence, "Multi-wavelength, all-solid-state, continuous wave mode locked picosecond Raman laser," Opt. Express **18**, 5289–5294 (2010).
11. F. Gérôme, P. Dupriez, J. Clowes, J. C. Knight, and W. J. Wadsworth, "High power tunable femtosecond soliton source using hollow-core photonic bandgap fiber, and its use for frequency doubling," Opt. Express **16**, 2381–2386 (2008).
12. S. M. Kobtsev, S. V. Kukarin, Y. S. Fedotov, and A. V. Ivanenko, "High-energy femtosecond 1086/543-nm fiber system for nano- and micromachining in transparent materials and on solid surfaces," Laser Phys. **21**, 308–311 (2011).

#211288 - $15.00 USD Received 1 May 2014; revised 27 Jun 2014; accepted 30 Jun 2014; published 14 Jul 2014

13. M. E. Fermann and I. Hartl, "Ultrafast Fiber Laser Technology," IEEE J. Sel. Top. Quantum Electron. **15**, 191–206 (2009).
14. D. Kielpinski, M. G. Pullen, J. Canning, M. Stevenson, P. S. Westbrook, and K. S. Feder, "Mode-locked picosecond pulse generation from an octave-spanning supercontinuum," Opt. Express **17**, 20833–20839 (2009).
15. K. Kieu, R. J. Jones, and N. Peyghambarian, "High power femtosecond source near 1 micron based on an all-fiber Er-doped mode-locked laser," Opt. Express **18**, 21350–21355 (2010).
16. G. Ycas, S. Osterman, and S. A. Diddams, "Generation of a 660-2100 nm laser frequency comb based on an erbium fiber laser," Opt. Lett. **37**, 2199–2201 (2012).
17. V. Pruneri, S. D. Butterworth, and D. C. Hanna, "Highly efficient green-light generation by quasi-phase-matched frequency doubling of picosecond pulses from an amplified mode-locked Nd:YLF laser," Opt. Lett. **21**, 390–392 (1996).
18. M. A. Arbore, M. M. Fejer, M. E. Fermann, A. Hariharan, A. Galvanauskas, and D. Harter, "Frequency doubling of femtosecond erbium-fiber soliton lasers in periodically poled lithium niobate," Opt. Lett. **22**, 13–15 (1997).
19. M. Hofer, M. E. Fermann, A. Galvanauskas, D. Harter, and R. S. Windeler, "High-power 100-fs pulse generation by frequency doubling of an erbium ytterbium-fiber master oscillator power amplifier," Opt. Lett. **23**, 1840–1842 (1998).
20. H. Zhu, T. Wang, W. Zheng, P. Yuan, L. Qian, and D. Fan, "Efficient second harmonic generation of femtosecond laser at one micron," Opt. Express **12**, 2150–2155 (2004).
21. Y. Furukawa, K. Kitamura, A. Alexandrovski, R. K. Route, M. M. Fejer, and G. Foulon, "Green-induced infrared absorption in MgO doped $LiNbO_3$," Appl. Phys. Lett. **78**, 1970–1972 (2001).
22. A. Bruner, D. Eger, M. B. Oron, P. Blau, M. Katz, and S. Ruschin, "Temperature-dependent Sellmeier equation for the refractive index of stoichiometric lithium tantalate," Opt. Lett. **28**, 194–196 (2003).
23. K. R. Parameswaran, J. R. Kurz, R. V. Roussev, and M. M. Fejer, "Observation of 99% pump depletion in single-pass second-harmonic generation in a periodically poled lithium niobate waveguide," Opt. Lett. **27**, 43–45 (2002).
24. O. A. Louchev, N. E. Yu, S. Kurimura, and K. Kitamura, "Thermal inhibition of high-power second-harmonic generation in periodically poled $LiNbO_3$ and $LiTaO_3$ crystals," Appl. Phys. Lett. **87**, 131101 (2005).
25. S. V. Tovstonog, S. Kurimura, I. Suzuki, K. Takeno, S. Moriwaki, N. Ohmae, N. Mio, and T. Katagai, "Thermal effects in high-power CW second harmonic generation in Mg-doped stoichiometric lithium tantalate," Opt. Express **16**, 11294–11299 (2008).
26. H. H. Lim, T. Katagai, S. Kurimura, T. Shimizu, K. Noguchi, N. Ohmae, N. Mio, and I. Shoji, "Thermal performance in high power SHG characterized by phase-matched calorimetry," Opt. Express **19**, 22588–22593 (2011).
27. A. Sahm, M. Uebernickel, K. Paschke, G. Erbert, and G. Tränkle, "Thermal optimization of second harmonic generation at high pump powers," Opt. Express **19**, 23029–23035 (2011).

1. Introduction

Lasers operating in the yellow-green region of the optical spectrum are a useful tool for a number of applications from atomic physics to biomedical science. The peak absorption wavelengths for various red fluorescent dyes and markers lie near 550 nm [1, 2], in addition to a number of resonances for atoms, such as Ba and Yb [3, 4], and molecules, such as hemoglobin and carbonylhemoglobin [5]. Additionally, ultrafast lasers operating within this region can be applied to two-photon fluorescence microscopy at short wavelengths. High repetition rate and average power are desirable in this application, in order to enable quick scanning, short timing resolution and a high signal to noise ratio [6].

A number of pulsed laser architectures, including frequency-doubled diode-pumped solid state lasers [7], Raman lasers [8–10] and fiber lasers [11, 12] have been developed to operate within this spectral region. Granados et al. have demonstrated a bulk-optics Raman laser able to deliver picosecond 559 nm pulses at Watt-level average power and a high repetition rate [9, 10]. Sub-picosecond pulses in the yellow-green region have also been demonstrated at high average power and repetition rates using the second harmonic of fiber lasers based on Yb-doped fiber (YDF) [11, 12]. Fiber lasers are versatile and relatively inexpensive laser sources that provide an attractive alternative to their bulk optic counterparts, in part due to the inherent stability of their all-fiber construction. However, the available wavelengths for fiber-based architectures in the yellow-green region have so far been limited to < 550 nm due to confinement of the fundamental wavelength to near 1.06 μm, the center of the YDF gain band [13].

#211288 - $15.00 USD Received 1 May 2014; revised 27 Jun 2014; accepted 30 Jun 2014; published 14 Jul 2014

We present a fiber-based source of picosecond pulses at 554 nm with 1.4 W average power and a 300 MHz pulse repetition rate. To our knowledge, this represents the first fiber-based picosecond pulse source in the yellow-green region that is able to operate at > 550 nm, while reaching Watt-level average power. These pulses are generated through single-pass second harmonic generation (SHG) from 1.11 μm pulses in periodically-poled stoichiometric $LiTaO_3$ (PPSLT). The picosecond 1.11 μm pulse train was produced from re-amplified supercontinuum generation, as demonstrated in several previous studies [14–16]. Using this supercontinuum architecture, coupled with highly efficient SHG, we have been able to overcome the wavelength restrictions on ultrafast fiber lasers, while maintaining favourable properties for applications such as two-photon microscopy.

A number of previous studies have shown high SHG efficiency using ultrafast picosecond and femtosecond fiber lasers using various types of nonlinear media [17–20]. Particular attention has been paid to nonlinear crystals capable of quasi-phase matching (QPM), such as PPSLT and periodically-poled $LiNbO_3$ (PPLN), due to their high nonlinearities and wide range of operating wavelengths [18, 19]. In this work, PPSLT was chosen in order to avoid the effects of photorefraction present at high intensities in PPLN [21, 22]. Without this inhibition, we have been able to achieve the generation of 1.4 W average power at 554 nm, with a conversion efficiency of 56% and the prospect of a further increase with greater available power at the fundamental wavelength.

2. Fundamental wavelength generation

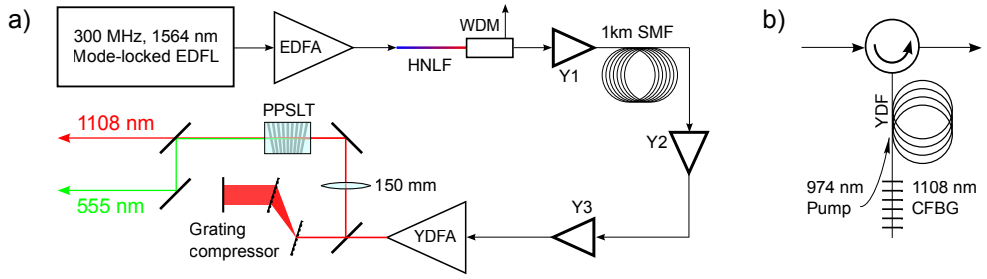

Fig. 1. (a) Schematic of experimental setup, showing mode-locked seed laser, supercontinuum generation and amplification stages in optical fiber. The three Yb-doped preamplifier stages are represented by Y1, Y2 and Y3. The pulse duration of the power YDFA output is compressed and the light is focused into an 11 mm fan-out PPSLT crystal. The fundamental and second harmonic are separated by two dichroic filters. (b) A detailed schematic of the 1108 nm preamplifier stages, consisting of a circulator, YDF and a chirped fiber Bragg grating (CFBG).

An Er-doped fiber laser, passively mode-locked at the fifth harmonic of the fundamental cavity repetition rate, was used to generate a 1564 nm pulse train with a repetition rate of 300 MHz. The amplified and compressed 55 fs pulses were used to generate supercontinuum spanning from 1.1 to >2 μm in Sumitomo highly nonlinear fiber with a nonlinear coefficient $\gamma = 0.02$ $W^{-1}m^{-1}$. The resulting supercontinuum was amplified and filtered in three YDF stages, as shown in Fig. 1 [14]. In each stage, the light passed through the gain fiber, was reflected at a chirped fiber Bragg grating (CFBG), and passed through the gain fiber again before exiting through the circulator. This arrangement maximized the gain in each stage while minimising amplified spontaneous emission (ASE). The reflection band of the CFBGs was centred at 1108.6 nm with bandwidth of 1 nm. A 1.15 km coil of SMF was used between

#211288 - $15.00 USD Received 1 May 2014; revised 27 Jun 2014; accepted 30 Jun 2014; published 14 Jul 2014

the first and second YDF preamplification stages to chirp the pulses to 20 ps. This length was selected by compromising between the nonlinearity of the pulses and the amount of dispersion that would require compensation. The preamplification stages provided a total of 27 mW of average power. As shown by Kielpinski et al. [14], there is no loss in coherence between the Er-doped seed laser and the amplified 1108.6 nm pulse train when using this technique. An IPG Photonics YAR-10K-1110-LP Yb-doped fiber power amplifier (YDFA) was used to amplify the resulting pulse train at 1108.6 nm to an average power of 5.0 W.

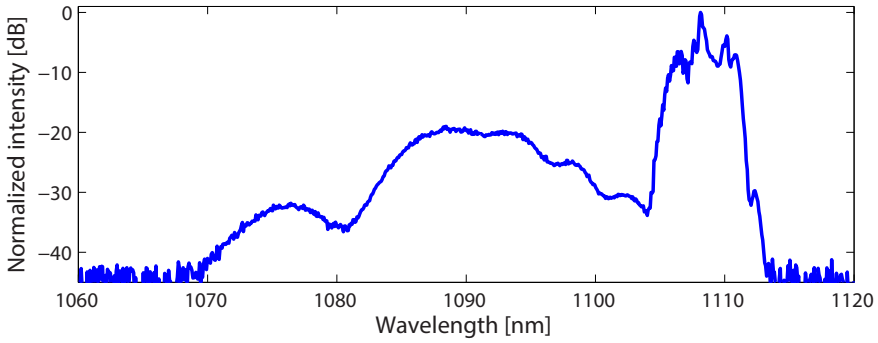

Fig. 2. Spectrum of 5 W YDFA output shown on a log scale, showing amplified spontaneous emission (ASE) centered at $\sim$ 1090 nm which accounts for $\sim$ 9% of the total power. The ASE is removed through spatial filtering in the grating compressor stage.

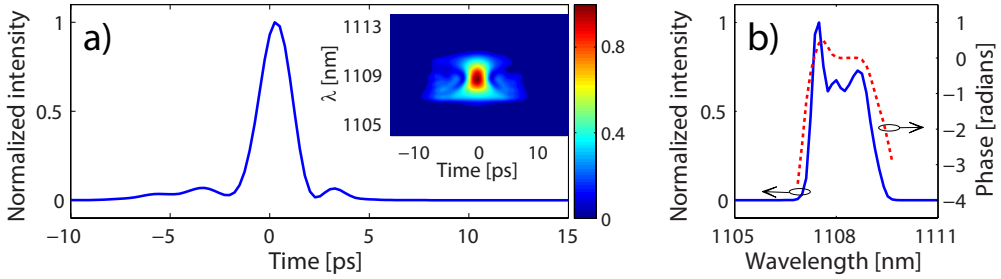

Fig. 3. (a) FROG trace (inset) and time domain retrieval of output pulse from grating compressor, giving a pulse duration of 1.9 ps. (b) Measured optical spectrum of IR pulse train (solid blue), with a center wavelength of 1108.1 nm and FWHM bandwidth of 1.72 nm. In addition, the spectral phase retrieved from the FROG (dashed red) is shown on the right axis.

The free-space output of the power YDFA was passed through a grating compressor using two LightSmyth LSFSG-1000 transmission gratings with a separation of 1.2 m, compressing the pulses to 1.9 ps in duration. ASE centered at $\sim$ 1090 nm accounts for $\sim$ 9% of the total YDFA output, as shown in Fig. 2, however this is removed through spatial filtering in the grating compressor stage. The pulse duration was measured by frequency resolved optical gating (FROG), using a MesaPhotonics FROGScan with an Ocean Optics HR4000 spectrometer, and a wavelength range of 503-577 nm. Figure 3 shows the FROG trace, pulse shape and spectrum determined from the FROG retrieval. The spectrum of the amplified IR pulse train is centred at 1108.1 nm with a FWHM bandwidth of 1.72 nm, broadened due to self-phase modulation (SPM) during amplification, giving a time-bandwidth product (TBWP) of 0.80. The relatively

#211288 - $15.00 USD Received 1 May 2014; revised 27 Jun 2014; accepted 30 Jun 2014; published 14 Jul 2014

large TBWP for a sech^2 pulse is due to the remaining non-quadratic component of the spectral phase, shown in Fig. 3, which was introduced by the SPM. As it is not quadratic in form, this phase could not be compensated further using the grating compressor. The effects of SPM on the IR spectrum and spectral phase show that higher peak powers cannot be reached in the current configuration, without further spectral broadening and distortion of the spectral phase.

The vertically polarized output of the grating compressor was focused down to a spot with an estimated 21.1 μm $1/e^2$ radius, inside the PPSLT crystal used for SHG, using a 150 mm focal length lens. The maximum available power was 2.52 W, giving a maximum available peak intensity of 0.24 GW/cm^2.

3. Second harmonic generation

The 11 mm long fan-out style PPSLT crystal was manufactured by Oxide Corporation and anti-reflection coated for both the fundamental and second harmonic wavelengths. Fan-out poling, with a period ranging from 8.8-9.7 μm, was chosen in order to quasi-phase match at 1108.6 nm, due to the lower cost and increased versatility compared to a single-period PPSLT designed for the same wavelength. The poling period of the PPSLT varies at a rate of 0.2 nm/μm over a full width of 5 mm, with a variation of $< 0.1\%$ over the $1/e^2$ diameter of the focused IR pump beam. As a result, we do not expect any significant effect on the phase-matching bandwidth as a result of the fan-out structure. The crystal temperature was held constant at 30.0 °C and the QPM period was tuned by translating the PPSLT orthogonally to the axis of beam propagation. The second harmonic was separated from the fundamental wavelength using two Semrock FF665-Di02 BrightLine filters, reducing the power of the fundamental light to $< 0.7\%$ of the remaining IR after the PPSLT, which is negligible compared to the SHG power.

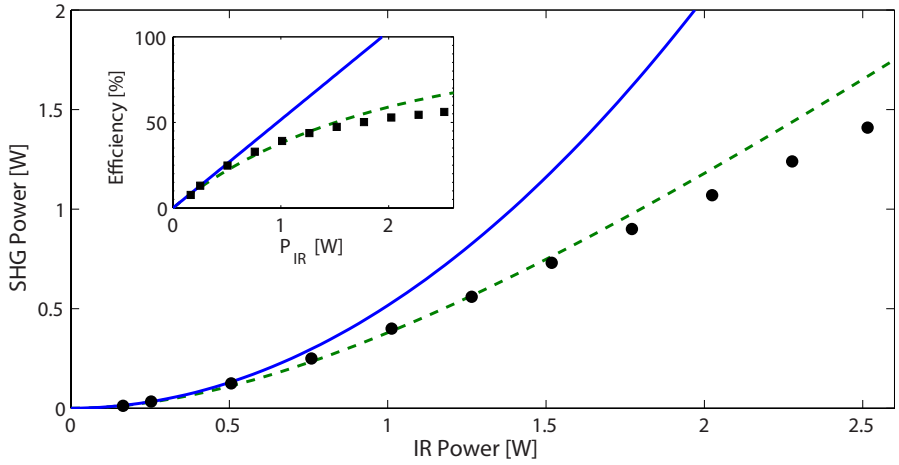

Fig. 4. SHG power (circles) and efficiency (squares, inset) plotted against fundamental power. A maximum SHG output of 1.41 W, at 56% efficiency is reached at an input power of 2.52 W. Using the maximum measured nonlinear efficiency of 51.6%/W, a quadratic estimate of SHG power levels and efficiencies (solid blue) and an estimate accounting for pump depletion (dashed green) are shown on both axes.

Figure 4 shows the measured SHG power and conversion efficiency, plotted against fundamental power, where a total of 1.41 W of SHG is produced from 2.52 W at the fundamental wavelength. We have found this average power level to be stable to within $\sim 5\%$ over several hours. The fundamental power was tuned continuously using a half waveplate and Glan laser

#211288 - $15.00 USD Received 1 May 2014; revised 27 Jun 2014; accepted 30 Jun 2014; published 14 Jul 2014

polarizer. The total conversion efficiency increases to 56% as the fundamental power increases to 2.52 W, where the efficiency is limited by the maximum available input power. No limitations due to photorefraction were observed using PPSLT, as compared to the presence of this problem at similar SHG power levels in PPLN.

Due to depletion of the pump beam the SHG power does not follow an ηP_0^2 relationship beyond small signal levels, as shown in Fig. 4. SHG under the effect of pump depletion can be estimated by

$$P_{SHG} = P_0 \tanh^2 \sqrt{\eta P_0} \tag{1}$$

where P_{SHG} and P_0 are the SHG and fundamental powers, and η is the small-signal nonlinear efficiency, in W^{-1} [23]. The maximum measured nonlinear efficiency $\eta = 51.6\%/W$ can be used to estimate the SHG performance with respect to quadratic and pump depletion models, as shown in Fig. 4. This illustrates that the SHG efficiency at higher fundamental power levels is below that expected by the estimate, even when accounting for pump depletion. However this additional reduction in efficiency can be explained by thermal effects which become evident at high pump intensity. Such thermal effects change the phase-matching conditions, thus reducing SHG efficiency [24], and could potentially be reduced using thermal optimization techniques [25–27]. However, thermal optimisation would become particularly important if scaling to higher fundamental power levels. These effects are independent of SHG power, showing that any contribution from photorefraction is negligible.

Figure 5 shows the autocorrelation trace and optical spectrum of the SHG pulses. We measured an autocorrelation duration of 4.10 ± 0.02 ps for the sech^2 pulses using an APE PulseCheck autocorrelator, ultimately giving a pulse duration of 2.66 ± 0.01 ps. The maximum peak power of the SHG pulses is therefore 1.36 ± 0.01 kW. We measured a center wavelength of 554.09 nm with a FWHM bandwidth of 0.19 nm, using the Ocean Optics HR4000 spectrometer used for the IR FROG measurements. The larger than expected TBWP of 0.49 is once again due to the higher-order spectral phase of the fundamental pulse, but we are unable to verify the spectral phase of the SHG pulse for comparison. The large reduction in the SHG spectral bandwidth, and resulting increase in pulse duration, is accounted for by the expected 0.27 nm phase matching bandwidth of the 11 mm long PPSLT crystal, as calculated from the group velocity mismatch.

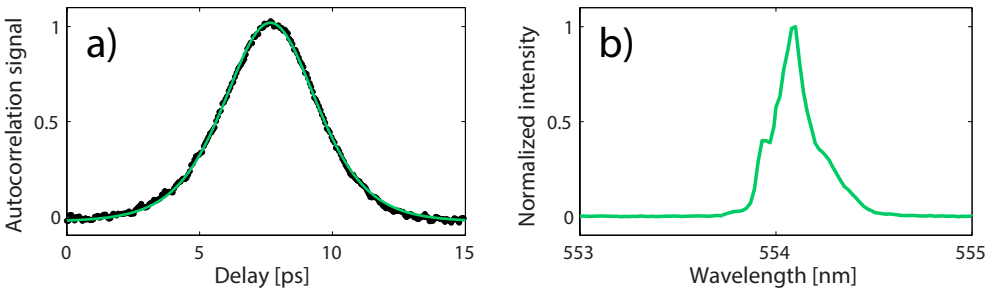

Fig. 5. (a) Autocorrelation trace of the second harmonic pulse. The solid line represents a sech^2 fit to the data, which gives a 2.66 ± 0.01 ps pulse duration. (b) Measured SHG spectrum, with 554.09 nm center wavelength and 0.19 nm FWHM bandwidth.

A time domain trace of the SHG pulse train is also shown in Fig. 6. The time domain signal was measured using a ThorLabs SV2-FC 2 GHz Si photodiode, coupled via multimode fiber, and recorded using an Agilent DSO8104A Oscilloscope with a bandwidth of 1 GHz. We observe a pulse to pulse amplitude variation of $< 5\%$.

#211288 - $15.00 USD Received 1 May 2014; revised 27 Jun 2014; accepted 30 Jun 2014; published 14 Jul 2014

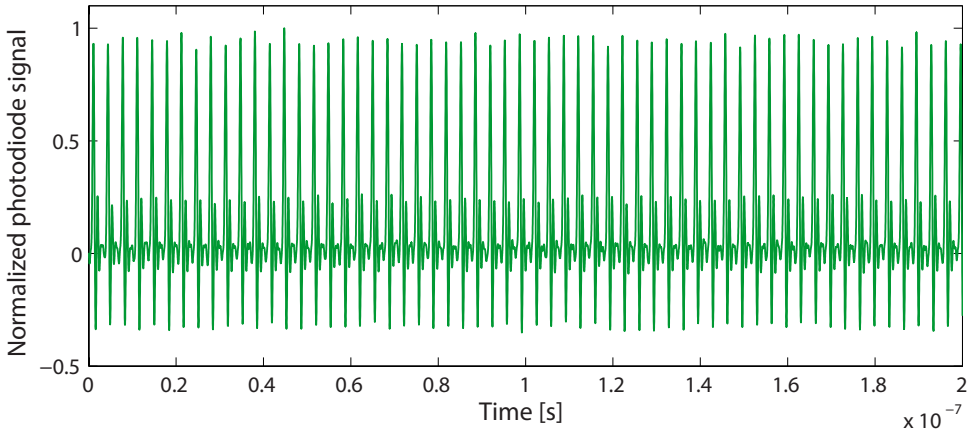

Fig. 6. Time domain photodiode trace of SHG pulse train, showing pulse to pulse amplitude variation of $< 5\%$.

4. Conclusion

We have demonstrated a source of 2.7 ps, 554 nm pulses at an average power of 1.41 W. The 554 nm pulse train was generated in PPSLT from the second harmonic of a 1.9 ps, 1.11 μm fiber laser source. 2.52 W of fundamental power was used, resulting in a total conversion efficiency of 56%, with a maximum nonlinear efficiency of 51.6%/W.

The design of the yellow-green pulse source is scalable to higher average power levels, as commercially available YDFAs can be made at considerably higher power levels, although consideration has to be taken for the distance from the YDF gain peak. In order to make the system more compact, the 1.2 m grating compressor could be replaced by hollow-core photonic crystal fiber to provide the anomalous dispersion required for compression of the amplified pulses. Additionally, gain in YDF is still present at wavelengths longer than those presented here, allowing for the center wavelength of the IR pulse train to be shifted up to 5 nm farther from the YDF gain peak, or indefinitely closer, without altering the design beyond the wavelength of the CFBG reflection band. This would allow for some versatility in the presented design to address applications of interest, or the fundamental flexibility of the supercontinuum-based design could be exploited to reach an even broader range of wavelengths.

Acknowledgments

This work was funded by the Australian Research Council (ARC) under DP130101613. D.K. was supported by an ARC Future Fellowship (FT110100513). M.S was supported by a Department of Industry Innovation Science and Research (DIISR) International Science Linkage (ISL) project CG130013 and J.C. by an ARC Future Fellowship (FT110100116).

#211288 - $15.00 USD Received 1 May 2014; revised 27 Jun 2014; accepted 30 Jun 2014; published 14 Jul 2014